

INTEGRITY ASSESSMENT OF THE BUTT WELD JOINT WITH DEFECT ACCORDING TO
EN ISO 6520-1, SERIES 400

PROCENA INTEGRITETA SUČEONOG ZAVAREN OG SPOJA SA GREŠKOM PREMA
EN ISO 6520-1, SERIJA 400

Originalni naučni rad / Original scientific paper
UDK /UDC: 621.791.05
Rad primljen / Paper received: 12.10.2016

Adresa autora / Author's address:

¹) J.J. Strossmayer University of Osijek, Mechanical Engng.
Faculty in Slavonski Brod, Slavonski Brod, Croatia
e-mail: dkozak@sfsb.hr

²) College of Slavonski Brod, Slavonski Brod, Croatia

Keywords

- welded joints
- butt weld
- finite element analysis
- fracture mechanics
- circumferential crack
- FAD diagram

Abstract

In this paper, a weld defect in the butt weld according to the EN ISO 6520-1, Series 400, is considered. By inspection of welds it is found that there are several joints with the same weld defect, but only the most critical is analysed. R6 procedure /1/ has been used to find critical depth of crack assuming that the crack is located on the whole butt weld circumferentially. The crack is assumed perpendicular to the vector of principal stress σ_1 at the location of its maximum. The stress which leads to the yielding of the remaining ligament and the corresponding stress intensity factor values are calculated by using finite element method based software. Characteristic fracture toughness values for pipe and elbow material are estimated from Charpy toughness. Several various crack depths are analysed, and all pairs of loading path points (K_r , L_r) lie in the safe area within the FAD diagram, so it is necessary to find the critical point of intersection with the material curve in the FAD diagram. It has been concluded that failure pressures equal limit pressures.

INTRODUCTION

Welded components are widely used in engineering; certain flaws located in welded joints may occur either in the process of welding or in the exploitation /2/. It is well known that the welded joint is a critical part of any welded component with respect to defects, geometry, misalignments and mechanical anisotropy. When cracks in welded joint are not considered, the International Institute of Welding (IIW) /3/ recommends three different linear-elastic methodologies to calculate the stress quantities to be used to estimate fatigue strength of welded components. First is the nominal stress approach, second is the hot-spot stress and third is solution with usage of the local stress fields determined by rounding the weld toe with a reference radius of 1 mm. In our considered case, the weld defect occurred prior to exploitation, so it is necessary to deter-

Ključne reči

- zavareni spojevi
- sučeoni šav
- analiza metodom konačnih elemenata
- mehanika loma
- obimska prslina
- FAD dijagram

Izvod

U ovom radu se razmatra greška u sučeonom šavu prema EN ISO 6520-1, Serija 400. Kontrolom šavova otkriveni su zavareni spojevi sa istom greškom u šavu, ali je samo najkritičnija analizirana. Primenjena je procedura R6 /1/ za određivanje kritične dubine prslina, pod pretpostavkom da se obimska prslina nalazi duž čitavog sučeonog šava. Pretpostavljen je normalan pravac prostiranja prslina u odnosu na vektor glavnog napona σ_1 u položaju njegovog maksimuma. Veličina napona, koji dovodi do tečenja preostalog ligamenta, kao i odgovarajuća veličina faktora intenziteta napona su određene upotrebom softvera na bazi metode konačnih elemenata. Karakteristične vrednosti žilavosti loma materijala cevi i kolena su određene Šarpi ispitivanjem žilavosti. Analizirano je nekoliko dubina prslina, a svi parovi tačaka krive opterećenja (K_r , L_r) se nalaze unutar bezbedne oblasti dijagrama FAD, stoga je potrebno odrediti kritičnu tačku preseka sa krivom otpornosti materijala u dijagramu FAD. Zaključuje se da su pritisci pri lomu jednaki graničnim pritiscima.

mine the integrity of the welded component, and the crack is considered at the location where it is most likely that it will appear.

According to the technical documentation received from the client, weld defects 401 – lack of fusion and 402 – lack of penetration (EN ISO 6520-1, Series 400) are considered in the butt weld of pipe and elbow, /4/. It is observed that one side of the root weld has not melted/welded through to full thickness. If the lack of fusion and the cracks are compared, it is evident that much more attention is paid to cracks, because the lack of fusion in many cases will lead to crack appearance. It is important to note that lack of fusion is as serious a defect as is a crack. Because of internal stresses produced during weld solidification and cooling, the faces sticking to each other will separate. Those gaps in the weld are very much like a crack, /4/.

Since this paper deals with a crack, in ref. /6-8/ some documents and papers deal with the lack of fusion.

Although in this study there are several joints with same defects (pipe-elbow and pipe-nozzle joints) only the most critical is analysed, being the butt weld between the pipe and elbow. This joint is considered critical, because the wall thickness of the elbow is less than the wall thickness of the nozzle.

GEOMETRY OF THE WELD GROOVE AND WELD DEFECT

Figure 1 shows the geometry of weld groove for pipe-elbow joint and Fig. 2 shows a simplified geometry of the weld defect.

As mentioned earlier, the weld defect is caused by 401 and 402 type imperfections. Taking this into account and based on the sketch of weld defect received from client, a 2D model for numerical FEM analysis is constructed. This model is shown in Fig. 2.

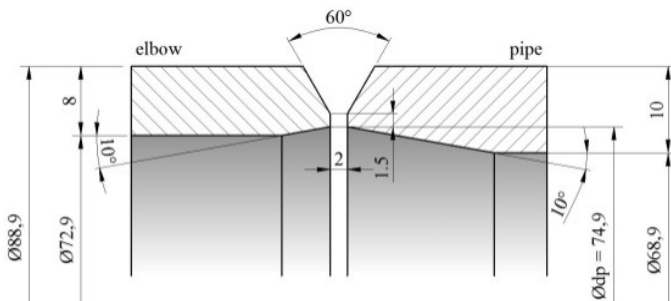


Figure 1. Geometry and dimensions of weld groove.

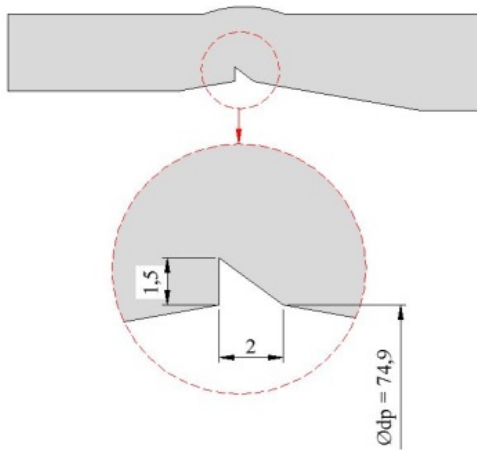


Figure 2. Geometry and dimensions of weld defect.

FINITE ELEMENT ANALYSIS OF WELD DEFECT

Stress analysis of weld defect is done by using commercial code for finite element analysis - Ansys. The model is

analysed for testing conditions (at room temperature $t_t = 20^\circ\text{C}$), where the internal pressure is $p = 7.94 \text{ MPa}$.

Material of pipe and elbow is 10 CrMo 9-10. The material is set as linear elastic-ideal plastic (Fig. 3) with Young's modulus $E = 185\,000 \text{ MPa}$ and Poisson's ratio $\nu = 0.3$. According to EN 10216-2:2002+A2:2007 (E), for the mentioned material at room temperature and for wall thickness $T < 16 \text{ mm}$, the proof strength is $R_{p0.2} = 280 \text{ MPa}$, /9/.

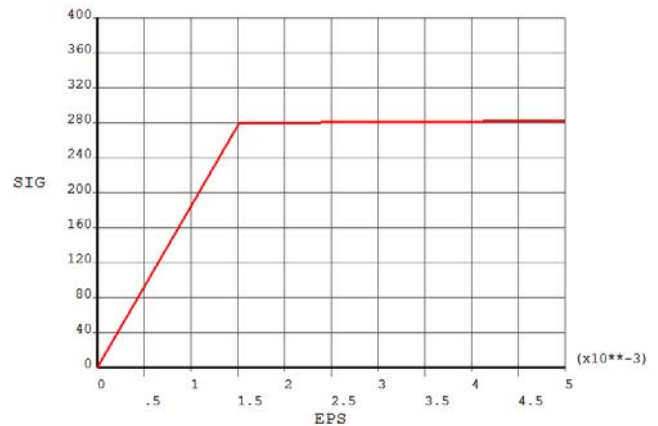


Figure 3. Material model for FEM analysis.

The problem is defined as 2D axisymmetric. The characteristic axisymmetric butt weld plane is discretized by axisymmetric element PLANE82 from Ansys library of elements, Fig. 4. This element provides more accurate results for mixed (quadrilateral-triangular) automatic meshing and can tolerate irregular shapes without much loss in accuracy. This 8-node element has compatible displacement shape and is well suited to model curved boundaries. It has two degrees of freedom at each node: translations in the nodal x and y directions, /10/.

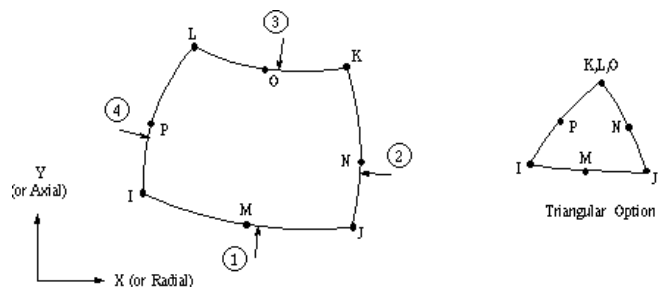


Figure 4. PLANE82 element geometry, /10/.

Figure 5 shows the finite element mesh with boundary conditions. The mesh consists of around 5800 elements and 17500 nodes. The mesh has been reached in density at places where stress concentration is expected.

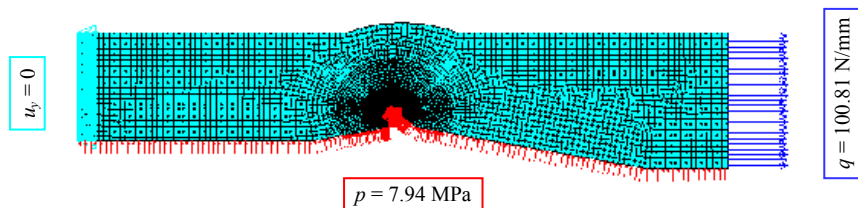


Figure 5. FEM mesh and boundary conditions

Besides the loading of internal pressure ($p_{EN}=7.94$ MPa), the longitudinal load q is also taken into consideration. Longitudinal load on the section of the pipe wall is calculated from the longitudinal forces caused by internal pressure, and from total weight of harps (taken from documentation) which is distributed to the single pipe. Furthermore, these two forces are added together and reduced to the 2D cross section of the pipe wall ($q = 100.81$ N/mm).

Results

The most interesting result from our point of view are the value and position of the principal stress σ_1 , since the crack appear perpendicular to σ_1 at the location of its maximum, Fig. 6.

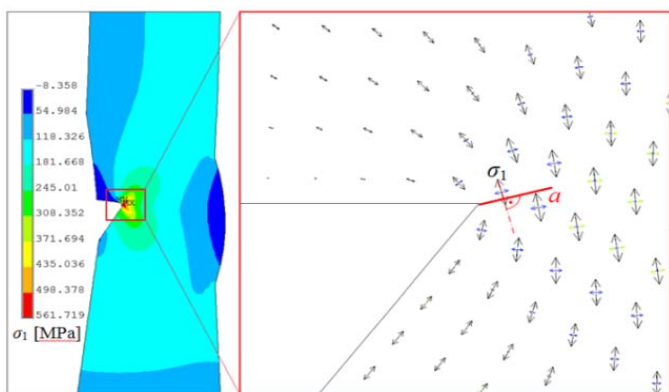


Figure 6. Crack appears perpendicular to the maximal principal stress σ_1 .

The crack is modelled as sharp in all cases of depth, with singular elements around the crack tip. The crack tip is defined as a place of stress concentration. It is necessary to calculate the stress and deformation distribution in the area of the crack tip, because those values are essential afterwards for calculating fracture mechanics parameters. Also, due to the need for limit pressure values (p_Y) for constructing the FAD diagram, these are calculated for various crack depths by using the finite element method.

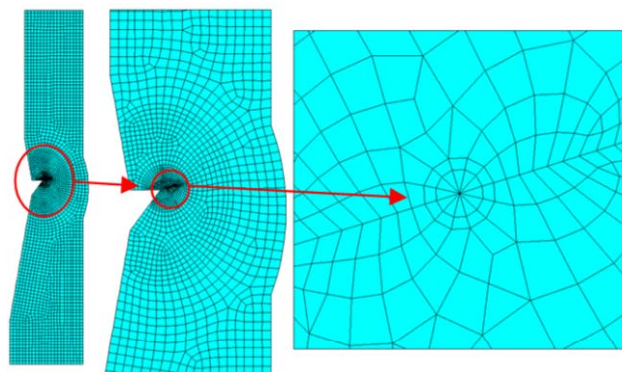


Figure 7. Finite element mesh with detail of singular elements around the crack tip.

A failure assessment procedure is performed by varying the crack depth as $a = 1; 2; 2.35$ and 2.4 mm. Figure 7 shows the finite element mesh with a detail of singular elements around the crack tip.

Critical depth of crack for internal pressure $p_{EN} = 7.94$ MPa is determined by constantly increasing depth of crack, a . It has been found that critical depth of crack is $a = 2.4$ mm (Fig. 8), which occurs when material yields through the remaining wall ligament.

Limit pressure values for mentioned crack depths are found starting from testing pressure ($p_{EN} = 7.94$ MPa) up to the value that causes plastic yielding through the ligament of the wall (Figs. 9, 10 and 11).

Limit pressure values obtained with failure assessment procedure for each crack depth are shown in Table 1. Failure pressure values for each case are found by using the FAD diagram.

Table 1. Values of limit pressure p_Y

a (mm)	p_Y (MPa)
1	12.7
2	9.6
2.35	8.2

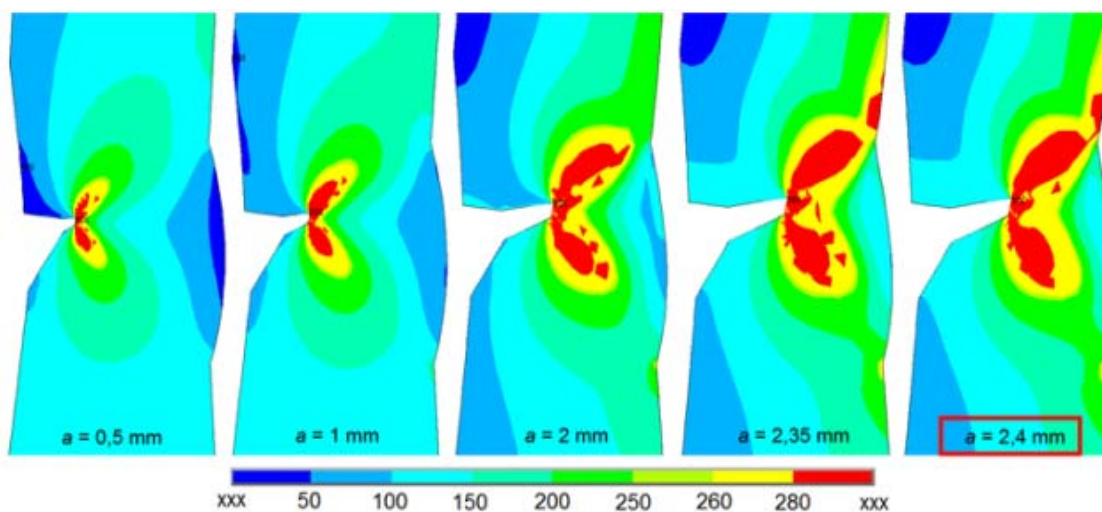


Figure 8. Critical depth of crack.

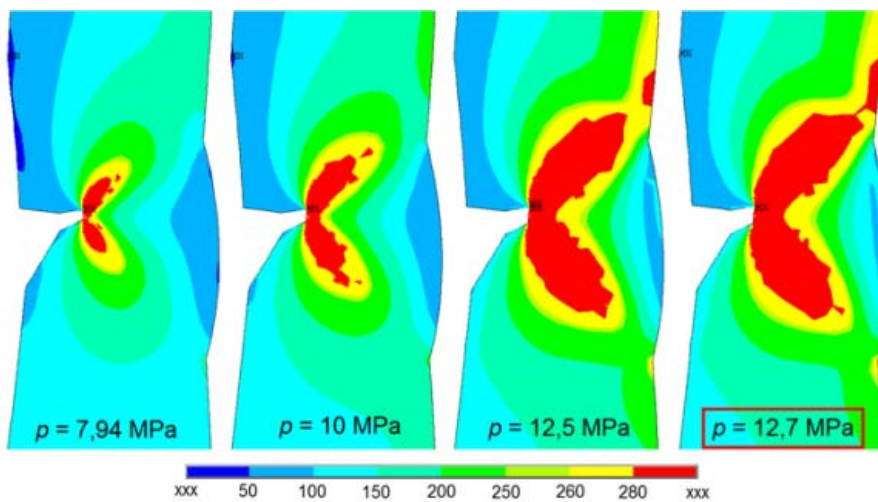


Figure 9. Yield zones spreading, $a = 1$ mm.

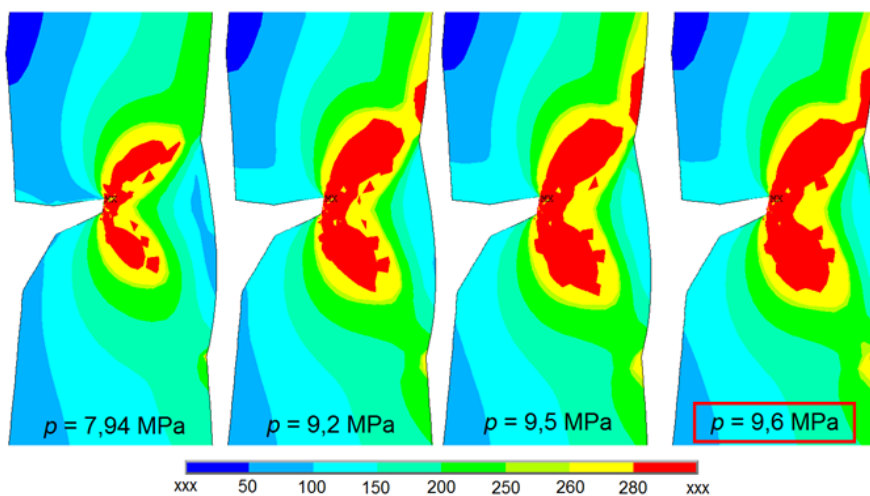


Figure 10. Yield zones spreading, $a = 2$ mm.

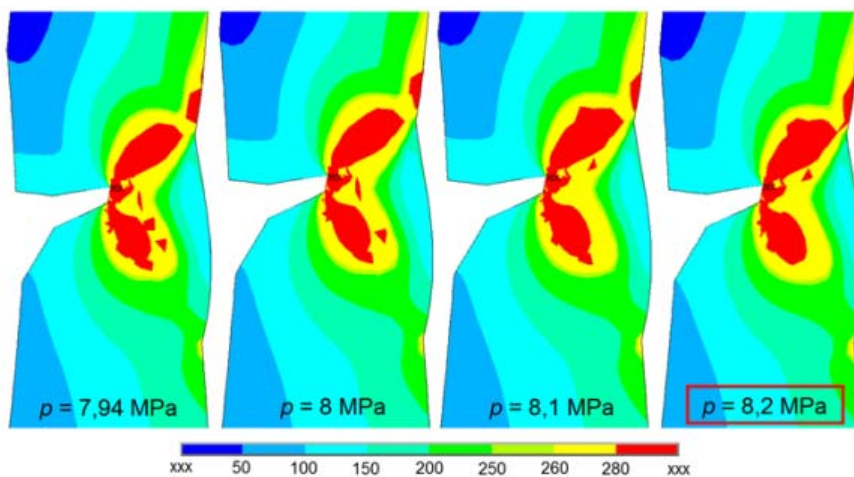


Figure 11. Yield zones spreading, $a = 2.35$ mm.

FAILURE ASSESSMENT DIAGRAM

Because the properties of material 10 CrMo 9-10 (toughness, yield- and ultimate tensile strength) are known, it is necessary to use SINTAP Basic Level 1, /11/.

For that case, the failure assessment diagram consists of three curves depicted by following equations (for material with Lüders plateau):

$$f(L_r) = \left(1 + \frac{1}{2} L_r^2\right)^{-\frac{1}{2}} \quad \text{for } L_r < 1 \quad (1)$$

$$f(1) = \left(\lambda + \frac{1}{2\lambda}\right)^{-\frac{1}{2}} \quad \text{for } L_r > 1 \quad (2)$$

where λ is:

$$\lambda = 1 + \frac{0,0375 \cdot E}{\sigma_Y} \cdot \left(\frac{1 - \sigma_Y}{1000} \right) \quad (3)$$

$$\text{for } 1 < L_r < L_r^{\max} = \frac{1}{2} \cdot \left(\frac{\sigma_Y + \sigma_U}{\sigma_Y} \right) \quad (5)$$

where N is the estimated strain hardening exponent, /11/:

$$f(L_r) = f(1) \cdot (L_r)^{\frac{N-1}{2N}} \quad (4) \quad N = 0,3 \cdot \left(1 - \frac{\sigma_Y}{\sigma_U} \right) \quad (6)$$

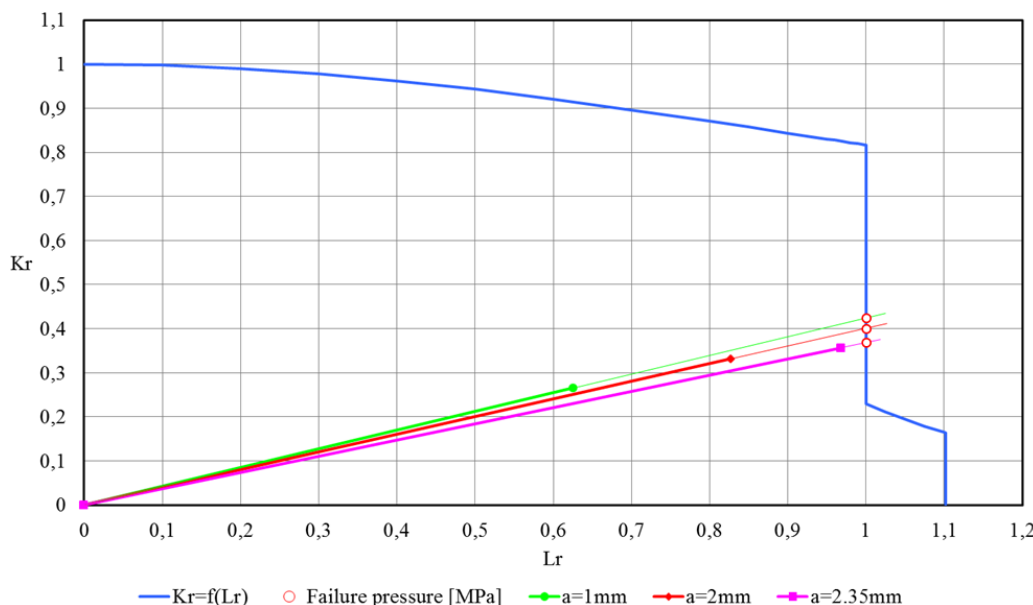


Figure 12. Failure assessment diagram (FAD), 10 CrMo 9-10

It is obvious from the FAD diagram (Fig. 12) that all crack loading paths intersect the material curve at the point of applied load to yield load ratio $L_r = 1$, practically. This means that failure pressure values of the cracked butt joint between pipe and elbow are equal to limit pressure values for analysed cases, /12/. It should be noted that the characteristic fracture toughness value K_{mat} is calculated from Charpy impact toughness value as $K_{mat} = 78.224 \text{ MPa} \cdot (\text{m})^{1/2}$, by using Eq.(7).

$$K_{mat} = \left[\left(12\sqrt{KV} - 20 \right) \cdot \left(\frac{25}{B} \right)^{1/4} \right] + 20 \quad (7)$$

CONCLUSIONS

Special attention has been given to the possibility that the surface circumferential crack could appear perpendicular to the principal stress σ_1 at the location of its maximum.

Critical depth of crack for testing conditions with internal pressure $p = 7.94 \text{ MPa}$ is found with the value of $a = 2.4 \text{ mm}$.

Limit pressure values are found by finite element method for three crack depths $a = 1; 2; 2.35 \text{ mm}$. As expected, the limit pressure p_Y decreases with increasing crack depth, a .

Corresponding FAD diagram has been constructed for the SINTAP Basic Level 1. Failure pressure values are equal to limit pressure values (all crack loading paths intersect the material curve at the point where $L_r = 1$), so there is no need for calculating the failure pressure from the FAD diagram by using the so-called ‘backward method’.

REFERENCES

1. R6, Revision 4, Assessment of the Integrity of Structures Containing Defects, British Energy Generation Ltd (BEG), Barnwood, Gloucester, 2000.
2. Konjatić, P., Kozak, D., Gubeljak, N. (2012), *The influence of the weld width on fracture behaviour of the heterogeneous welded joint*. Key Engng. Mater., 367-370. doi:10.4028/www.scientific.net/KEM.488-489.367
3. Hobbacher, A. (2007), *Recommendations for fatigue design of welded joints and components*. IIW document XIII-2151-07/ XV-1254-07.
4. Denys, R. (2000), Pipeline Technology: Proc. 3rd Int. Pipeline Technology Conference, Brugge, Belgium.
5. Rihar, G. (2000), *Lack of fusion in welded joints*. 15th World Conf. on Non-Destructive Testing. 15-21 Oct. 2000, Rome.
6. Yamauchi, N., Inaba, Y., Taka, T. (1982), *Formation mechanism of lack of fusion in MAG welding*. IIW document 212-529-82.
7. Pomaska, H.U. (1983), *Causes for weld defects*. IIW document XII-B-046-83.
8. Rihar, G., Uran, M. (2006), IIW-1698-05 (ex-doc. V-1285-04) Lack of fusion - Characterisation of indications. *Welding in the World*, 50, 1/2, 35-39.
9. EN 10216-2:2002+A2:2007 (E).
10. ANSYS Release 12.1, Help Topics.
11. Kim, Y.-J. (1998), *Comparison: various levels of the SINTAP procedure for homogeneous structures*. GKSS.
12. Kozak, D., Konjatić, P., Matejiček, F., Damjanović, D. (2010), *Weld misalignment influence on the structural integrity of cylindrical pressure vessel*. *Struc. Int. and Life*, 153.-159.